CHAPTER 12
STRENGTH UNDER STATIC CIRCUMSTANCES

Charles R. Mischke, Ph.D., P.E.
Professor Emeritus of Mechanical Engineering
Iowa State University
Ames, Iowa

Joseph E. Shigley
Professor Emeritus
The University of Michigan
Ann Arbor, Michigan

GLOSSARY OF SYMBOLS

a	Crack semilength
A	Area
D, d	Diameter
F	Force or load
I	Second moment of area
J	Second polar moment of area
K	Stress-intensity factor
K'	Stress-concentration factor for static loading
K_c	Critical-stress-intensity factor
K_t	Normal-stress-concentration factor
K_{ts}	Shear-stress-concentration factor
M	Moment
n	Design factor
q_s	Sensitivity index

r	Radius or ratio
S_{sy}	Yield strength in shear
S_{uc}	Ultimate compressive strength
S_{ut}	Ultimate tensile strength
S_y	Yield strength
η	Factor of safety
σ	Normal stress
σ'	von Mises stress
τ	Shear stress
τ_o	Octahedral shear stress or nominal shear stress

12.1 PERMISSIBLE STRESSES AND STRAINS

The discovery of the relationship between stress and strain during elastic and plastic deformation allows interpretation either as a stress problem or as a strain problem. Imposed conditions on machine elements are more often loads than deformations, and so the usual focus is on stress rather than strain. Consequently, when durability under static conditions is addressed, attention to permissible stress is more common than attention to permissible strain.

Permissible stress levels are established by

- Experience with successful machine elements
- Laboratory simulations of field conditions
- Corporate experience manifested as a design-manual edict
- Codes, standards, and state of the art

During the design process, permissible stress levels are established by dividing the significant strength by a *design factor n*. The design factor represents the original intent or goal. As decisions involving discrete sizes are made, the stress levels depart from those intended. The quotient, obtained by dividing the significant strength by the load-induced stress at the critical location, is the *factor of safety* η, which is unique to the completed design. The design factor represents the goal and the factor of safety represents attainment. The adequacy assessment of a design includes examination of the factor of safety. Finding a permissible stress level which will provide satisfactory service is not difficult. Competition forces a search for the highest stress level which still permits satisfactory service. This is more difficult.

Permissible stress level is a function of material strength, which is assessible only by test. Testing is costly. Where there is neither time nor money available or testing the part is impossible, investigators have proposed theories of failure for guidance of designers. Use of a theory of failure involves (1) identifying the significant stress at the critical location and (2) comparing that stress condition with the strength of the part at that location in the condition and geometry of use. Standardized tests, such as the simple tension test, Jominy test, and others, provide some of the necessary information. For example, initiation of general yielding in a ductile part is predicted on the basis of yield strength exhibited in the simple tension test and modified by the manufacturing process. Rupture of brittle parts is predicted on the basis of ultimate strength (see Chap. 8).

Estimates of permissible stress level for long and satisfactory performance of function as listed above are based on design factors reflecting these experiences and are modified by the following:

1. Uncertainty as to material properties within a part, within a bar of steel stock, and within a heat of steel or whatever material is being considered for the design. Properties used by a designer may come not from an actual test, but from historical experience, since parts are sometimes designed before the material from which they will be made has even been produced.
2. Uncertainty owing to the discrepancy between the designed part and the necessarily small size of the test specimen. The influence of size on strength is such that smaller parts *tend* to exhibit larger strengths.
3. Uncertainty concerning the actual effects of the manufacturing process on the local material properties at the critical locations in the part. Processes such as upsetting, cold or hot forming, heat treatment, and surface treatment change strengths and other properties.
4. Uncertainties as to the true effect of peripheral assembly operations on strengths and other properties. Nearby weldments, mechanical fasteners, shrink fits, etc., all have influences that are difficult to predict with any precision.
5. Uncertainty as to the effect of elapsed time on properties. Aging in steels, aluminums, and other alloys occurs, and some strengthening mechanisms are time-dependent. Corrosion is another time-dependent enemy of integrity.
6. Uncertainty as to the actual operating environment.
7. Uncertainty as to the validity and precision of the mathematical models employed in reaching decisions on the geometric specifications of a part.
8. Uncertainty as to the intensity and dispersion of loads that may or will be imposed on a machine member and as to the understanding of the effect of impact.
9. Uncertainty as to the stress concentrations actually present in a manufactured part picked at random for assembly and use. Changes in tool radius due to wear, regrinding, or replacement can have a significant influence on the stress levels actually attained in parts in service.
10. Company design policies or the dictates of codes.
11. Uncertainty as to the completeness of a list of uncertainties.

Although specific recommendations that suggest design factors qualified by usage are to be found in many places, such factors depend on the stochastic nature of properties, loading, geometry, the form of functional relationships between them, and the reliability goal.

12.2 THEORY OF STATIC FAILURE

For ductile materials, the best estimation method for predicting the onset of yielding, for materials exhibiting equal strengths in tension and compression, is the octahedral shear theory (distortion energy or Hencky-von Mises). The *octahedral shear stress* is

$$\tau_o = \tfrac{1}{3}[(\sigma_1 - \sigma_2)^2 + (\sigma_2 - \sigma_3)^2 + (\sigma_3 - \sigma_1)^2]^{1/2}$$

where σ_1, σ_2, and σ_3 are ordered principal stresses (see Chap. 49). In terms of orthogonal stress components in any other directions, the octahedral shear stress is

$$\tau_o = \tfrac{1}{3}\left[(\sigma_x - \sigma_y)^2 + (\sigma_y - \sigma_z)^2 + (\sigma_z - \sigma_x)^2 + 6(\tau_{xy}^2 + \tau_{yz}^2 + \tau_{zx}^2)\right]^{1/2}$$

The limiting value of the octahedral shear stress is that which occurs during uniaxial tension at the onset of yield. This limiting value is

$$\tau_o = \frac{\sqrt{2}S_y}{3}$$

By expressing this in terms of the principal stresses and a design factor, we have

$$\frac{S_y}{n} = \frac{3}{\sqrt{2}}\,[\tau_o]_{\text{lim}} = \frac{1}{\sqrt{2}}[(\sigma_1 - \sigma_2)^2 + (\sigma_2 - \sigma_3)^2 + (\sigma_3 - \sigma_1)^2]^{1/2} = \sigma' \qquad (12.1)$$

The term σ' is called the *von Mises stress.* It is the uniaxial tensile stress that induces the same octahedral shear (or distortion energy) in the uniaxial tension test specimen as does the triaxial stress state in the actual part.

For plane stress, one principal stress is zero. If the larger nonzero principal stress is σ_A and the smaller σ_B, then

$$\sigma' = (\sigma_A^2 + \sigma_B^2 - \sigma_A\sigma_B)^{1/2} = \frac{S_y}{n} \qquad (12.2)$$

By substituting the relation

$$\sigma_{A,B} = \frac{\sigma_x - \sigma_y}{2} \pm \sqrt{\left(\frac{\sigma_x - \sigma_y}{2}\right)^2 + \tau_{xy}^2}$$

we get a more convenient form:

$$\sigma' = (\sigma_x^2 + \sigma_y^2 - \sigma_x\sigma_y + 3\tau_{xy}^2)^{1/2} = \frac{S_y}{n} \qquad (12.3)$$

Example 1. A thin-walled pressure cylinder has a tangential stress of σ and a longitudinal stress of $\sigma/2$. What is the permissible tangential stress for a design factor of n?

Solution

$$\sigma' = (\sigma_A^2 + \sigma_B^2 - \sigma_A\sigma_B)^{1/2}$$

$$= \left[\sigma^2 + \left(\frac{\sigma}{2}\right)^2 - \sigma\left(\frac{\sigma}{2}\right)\right]^{1/2} = \frac{S_y}{n}$$

From which

$$\sigma = \frac{2}{\sqrt{3}}\,\frac{S_y}{n}$$

Note especially that this result is larger than the uniaxial yield strength divided by the design factor.

Example 2. Estimate the shearing yield strength from the tensile yield strength.
Solution. Set $\sigma_A = \tau$, $\sigma_B = -\tau$, and at yield, $\tau = S_{sy}$, so

$$\sigma' = (\sigma_A^2 + \sigma_B{}^2 - \sigma_A\sigma_B)^{1/2}$$
$$= [S_{sy}^2 + (-S_{sy})^2 - S_{sy}(-S_{sy})]^{1/2} = S_y$$

Solving gives

$$S_{sy} = \frac{S_y}{\sqrt{3}} = 0.577S_y$$

12.2.1 Brittle Materials

To define the criterion of failure for brittle materials as *rupture,* we require that the fractional reduction in area be less than 0.05; this corresponds to a true strain at fracture of about 0.05. Brittle materials commonly exhibit an ultimate compressive strength significantly larger than their ultimate tensile strength. And unlike with ductile materials, the ultimate torsional strength is approximately equal to the ultimate tensile strength. If σ_A and σ_B are ordered-plane principal stresses, then there are five points on the rupture locus in the $\sigma_A\sigma_B$ plane that can be immediately identified (Fig. 12.1). These are

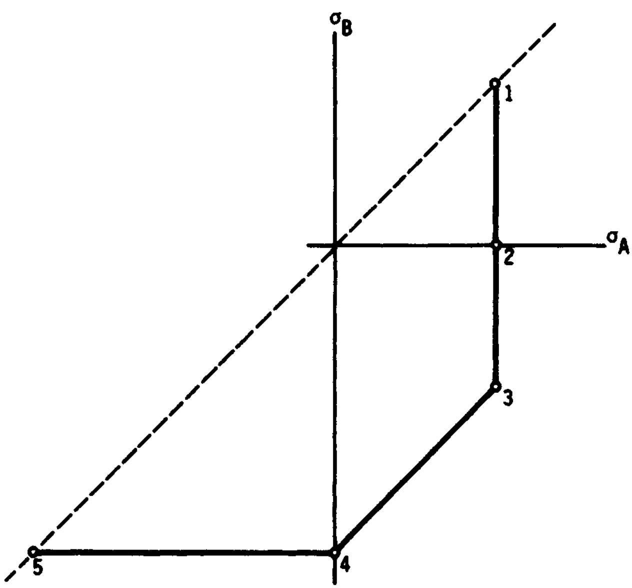

FIGURE 12.1 $\sigma_A\sigma_B$ plane with straight-line Coulomb-Mohr strength locus.

Locus 1–2: $\sigma_A = S_{ut}, \sigma_A > \sigma_B > 0$

Point 3: $\sigma_A = S_{ut} = S_{su}, \sigma_B = -S_{ut} = -S_{su}$

Point 4: $\sigma_A = 0, \sigma_B = S_{uc}$

Locus 4–5: $\sigma_B = S_{uc}, \sigma_A < 0$

Connecting points 2, 3, and 4 with straight-line segments defines the *modified Mohr theory of failure.* This theory evolved from the *maximum normal stress theory* and the *Coulomb-Mohr internal friction theory.* We can state this in algebraic terms by defining $r = \sigma_B/\sigma_A$. The result is

$$\sigma_A = \frac{S_{ut}}{n} \qquad \text{when } \sigma_A > 0, \sigma_B > -\sigma_A$$

$$\sigma_A = \frac{S_{uc}S_{ut}/n}{(1+r)S_{ut} + S_{uc}} \qquad \text{when } \sigma_A > 0, \sigma_B < 0, r < -1 \tag{12.4}$$

$$\sigma_B = \frac{S_{uc}}{n} \qquad \text{when } \sigma_A < 0$$

Figure 12.2 shows some experimental points from tests on gray cast iron.

Example 3. A ¼-in-diameter ASTM No. 40 cast iron pin with S_{ut} = 40 kpsi and S_{uc} = −125 kpsi is subjected to an axial compressive load of 800 lb and a torsional moment of 100 lb · in. Estimate the factor of safety.

Solution. The axial stress is

$$\sigma_x = \frac{F}{A} = \frac{-800}{\pi(0.25)^2/4} = -16.3 \text{ kpsi}$$

The surface shear stress is

$$\tau_{xy} = \frac{16T}{\pi d^3} = \frac{16(100)}{\pi(0.25)^3} = 32.6 \text{ kpsi}$$

The principal stresses are

$$\sigma_{A,B} = \frac{\sigma_x + \sigma_y}{2} \pm \sqrt{\left(\frac{\sigma_x - \sigma_y}{2}\right)^2 + \tau_{xy}^2}$$

$$= \frac{-16.3}{2} \pm \sqrt{\left(\frac{-16.3}{2}\right)^2 + (32.6)^2} = 25.45, -41.25 \text{ kpsi}$$

$$r = \frac{\sigma_B}{\sigma_A} = \frac{-41.25}{25.45} = -1.64$$

The rupture line is the 3–4 locus, and the factor of safety is

$$\eta = \frac{S_{uc}S_{ut}}{(1+r)S_{ut} + S_{uc}} \frac{1}{\sigma_A}$$

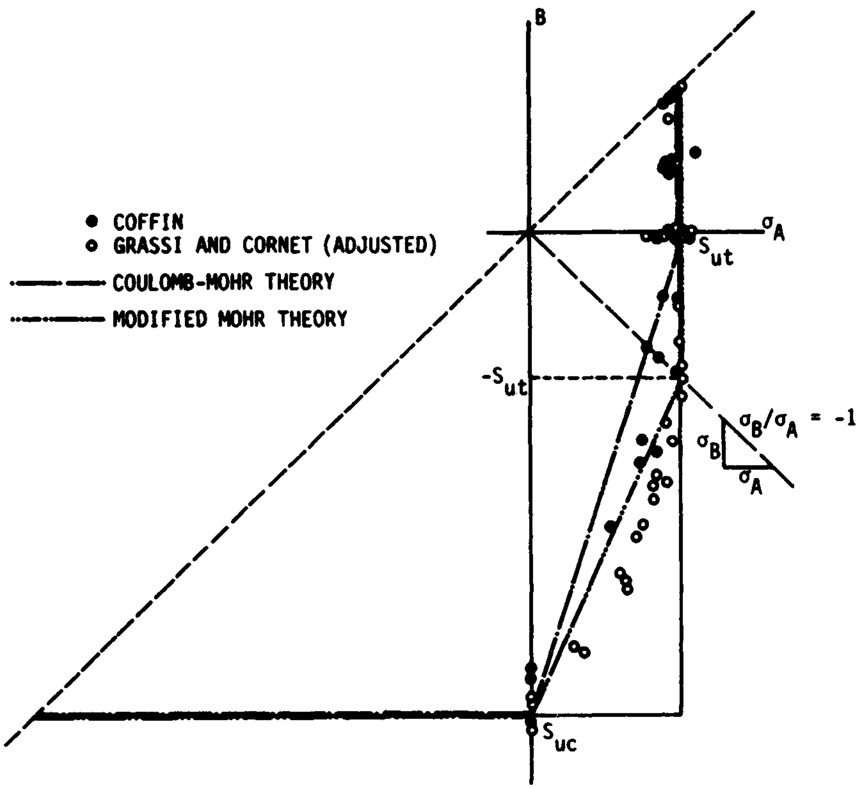

FIGURE 12.2 Experimental data from tests of gray cast iron subjected to biaxial stresses. The data were adjusted to correspond to $S_{ut} = 32$ kpsi and $S_{uc} = 105$ kpsi. Superposed on the plot are graphs of the maximum-normal-stress theory, the Coulomb-Mohr theory, and the modified Mohr theory. (*Adapted from J. E. Shigley and L. D. Mitchell,* Mechanical Engineering Design, *4th ed., McGraw-Hill, 1983, with permission.*)

$$= \frac{(-125)(40)}{[(1-1.64)(40)-125](25.45)} = 1.30$$

12.3 STRESS CONCENTRATION

Geometric discontinuities increase the stress level beyond the nominal stresses, and the elementary stress equations are inadequate estimators. The geometric discontinuity is sometimes called a *stress raiser,* and the domains of departure from the elementary equation are called the *regions of stress concentration.* The multiplier applied to the nominal stress to estimate the peak stress is called the *stress-concentration factor,* denoted by K_t or K_{ts}, and is defined as

$$K_t = \frac{\sigma_{max}}{\sigma_o} \qquad K_{ts} = \frac{\tau_{max}}{\tau_o} \tag{12.5}$$

respectively. These factors depend solely on part geometry and manner of loading and are independent of the material. Methods for determining stress-concentration factors include theory of elasticity, photoelasticity, numerical methods including finite elements, gridding, brittle lacquers, brittle models, and strain-gauging techniques.

Peterson [12.1] has been responsible for many useful charts. Some charts representing common geometries and loadings are included as Figs. 12.3 through 12.17. The user of any such charts is cautioned to use the nominal stress equation upon which the chart is based.

When the region of stress concentration is small compared to the section resisting the static loading, localized yielding in ductile materials limits the peak stress to the approximate level of the yield strength. The load is carried without gross plastic distortion. The stress concentration does no damage (strain strengthening occurs), and it can be ignored. No stress-concentration factor is applied to the stress. For low-ductility materials, such as the heat-treated and case-hardened steels, the full geometric stress-concentration factor is applied unless notch-sensitivity information to the contrary is available. This notch-sensitivity equation is

$$K' = 1 + q_s(K_t - 1) \tag{12.6}$$

where K' = the actual stress-concentration factor for static loading and q_s = an index of sensitivity of the material in static loading determined by test. The value of q_s for hardened steels is approximately 0.15 (if untempered, 0.25). For cast irons, which have internal discontinuities as severe as the notch, q_s approaches zero and the full value of K_t is rarely applied.

Kurajian and West [12.3] have derived stress-concentration factors for hollow stepped shafts. They develop an equivalent solid stepped shaft and then use the usual charts (Figs. 12.10 and 12.11) to find K_t. The formulas are

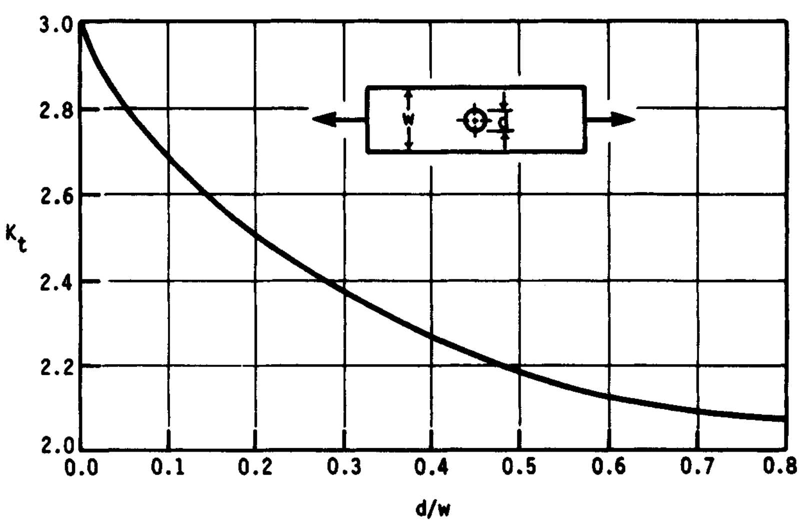

FIGURE 12.3 Bar in tension or simple compression with a transverse hole. $\sigma_o = F/A$, where $A = (w - d)t$, and t = thickness. *(From Peterson [12.2].)*

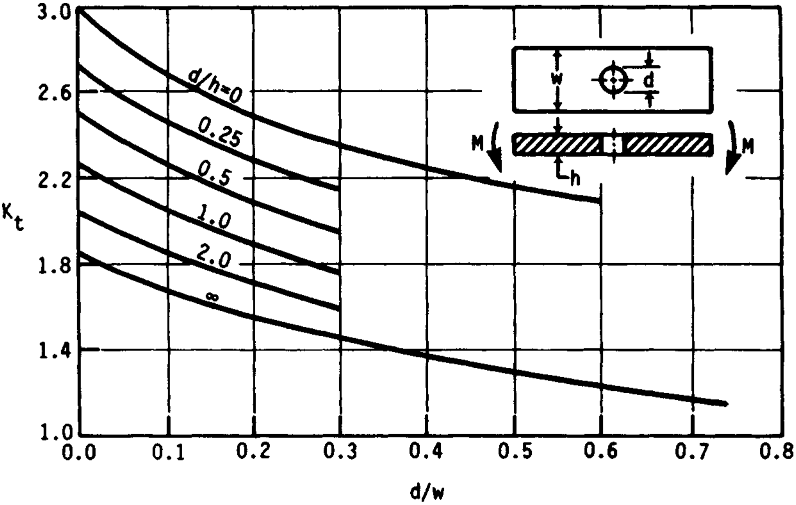

FIGURE 12.4 Rectangular bar with a transverse hole in bending. $\sigma_o = Mc/I$, where $I = (w - d)h^3/12$. *(From Peterson [12.2].)*

$$D = \left(\frac{D_o^4 - d_i^4}{D_o}\right)^{1/3} \qquad d = \left(\frac{d_o^4 - d_i^4}{d_o}\right)^{1/3} \tag{12.7}$$

where D, d = diameters of solid stepped shaft (Fig. 12.10)
D_o, d_o = diameters of hollow stepped shaft
d_i = hole diameter

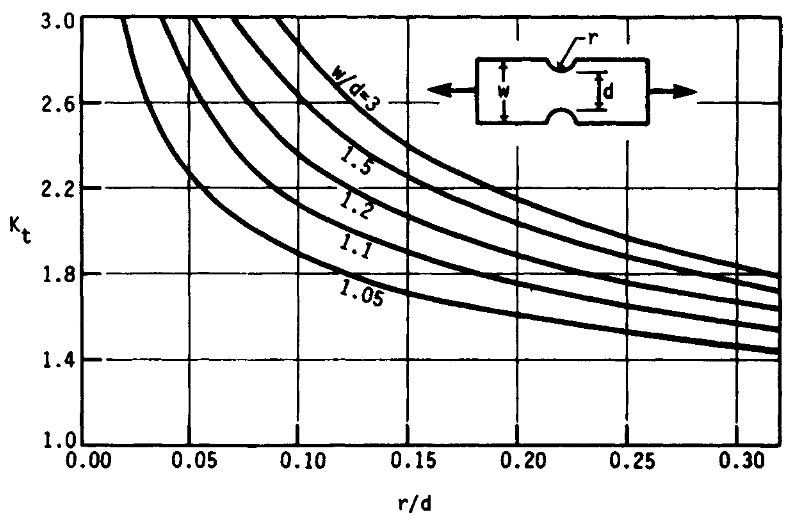

FIGURE 12.5 Notched rectangular bar in tension or simple compression. $\sigma_o = F/A$, where $A = td$ and t = thickness. *(From Peterson [12.2].)*

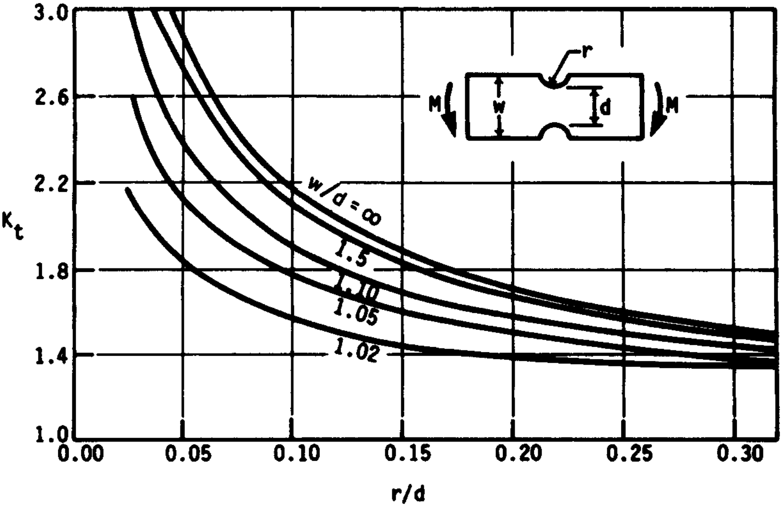

FIGURE 12.6 Notched rectangular bar in bending. $\sigma_o = Mc/I$, where $c = d/2, I = td^3/12$, and t = thickness. *(From Peterson [12.2].)*

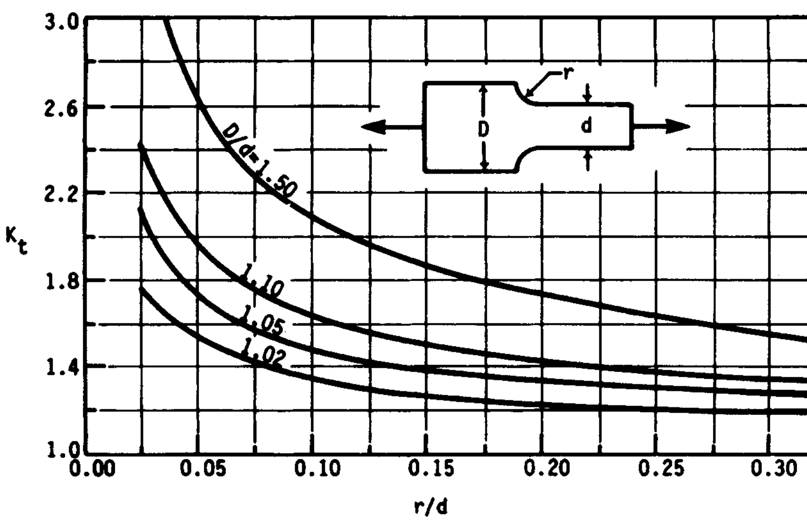

FIGURE 12.7 Rectangular filleted bar in tension or simple compression. $\sigma_o = F/A$, where $A = td$ and t = thickness. *(From Peterson [12.2].)*

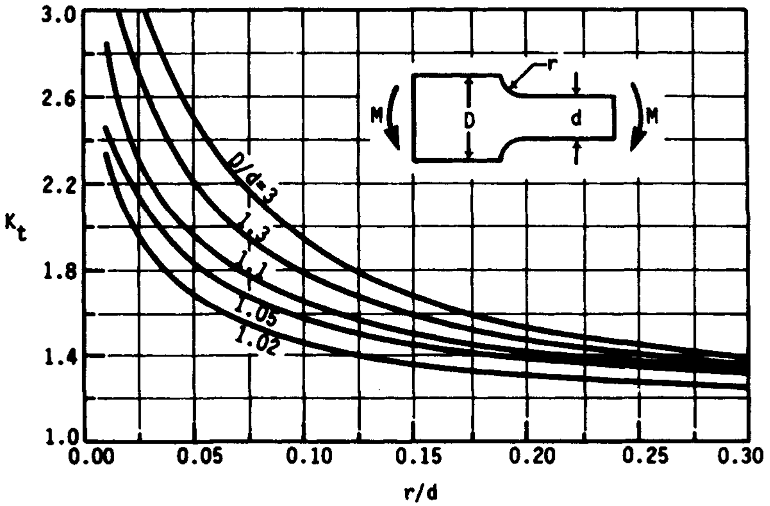

FIGURE 12.8 Rectangular filleted bar in bending. $\sigma_o = Mc/I$, where $c = d/2$, $I = td^3/12$, and t = thickness. *(From Peterson [12.2].)*

The fillet radius is unchanged. No change is necessary for axial loading because of the uniform stress distribution.

12.4 FRACTURE MECHANICS

The use of stress-concentration factors is really of little use when brittle materials are used or when a very small crack or flaw exists in the material. Ductile materials

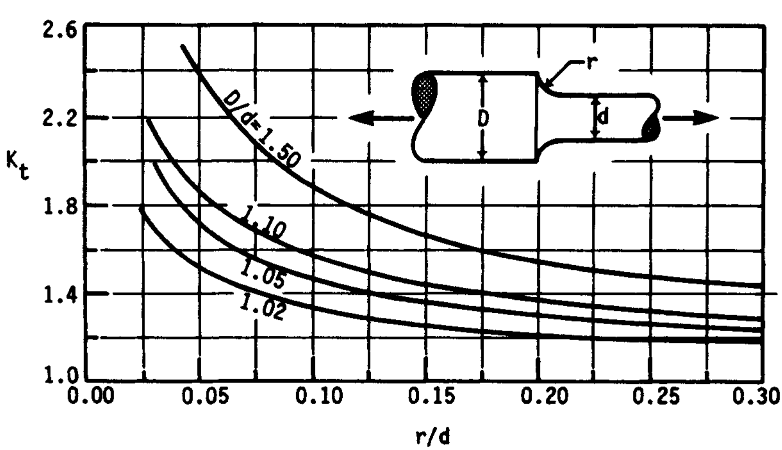

FIGURE 12.9 Round shaft with shoulder fillet in tension. $\sigma_o = F/A$, where $A = \pi d^2/4$. *(From Peterson [12.2].)*

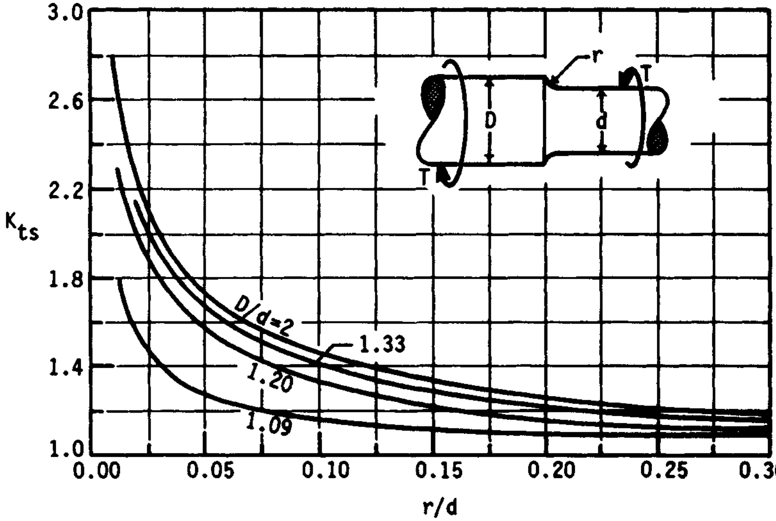

FIGURE 12.10 Round shaft with shoulder fillet in torsion. $\tau_o = Tc/J$, where $c = d/2$ and $J = \pi d^4/32$. *(From Peterson [12.2].)*

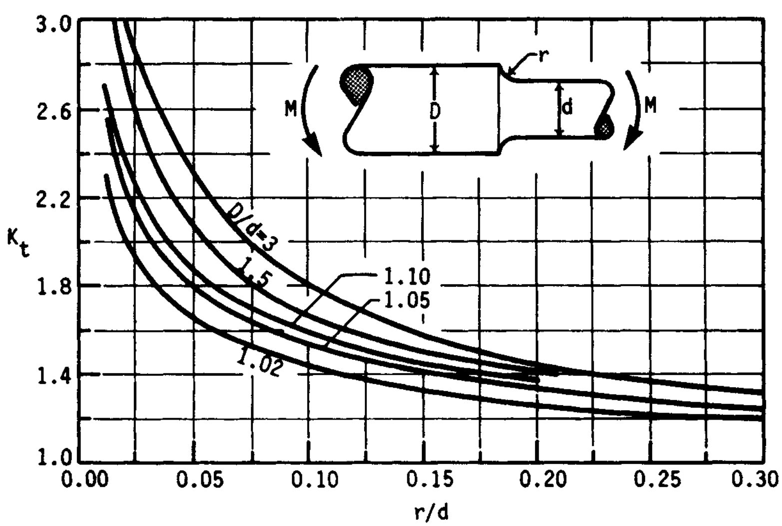

FIGURE 12.11 Round shaft with shoulder fillet in bending. $\sigma_o = Mc/I$, where $c = d/2$ and $I = \pi d^4/64$. *(From Peterson [12.2].)*

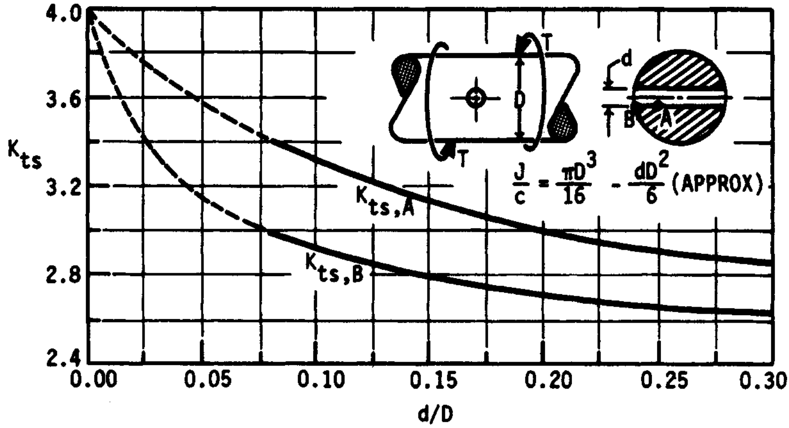

FIGURE 12.12 Round shaft in torsion with transverse hole. *(From Peterson [12.2].)*

also may fail in a brittle manner, possibly because of low temperature or other causes. So another method of analysis is necessary for all materials that cannot yield and relieve the stress concentration at a notch, defect, or crack.

Fracture mechanics can be used to determine the average stress in a part that will cause a crack to grow; energy methods of analysis are used (see Ref. [12.4]).

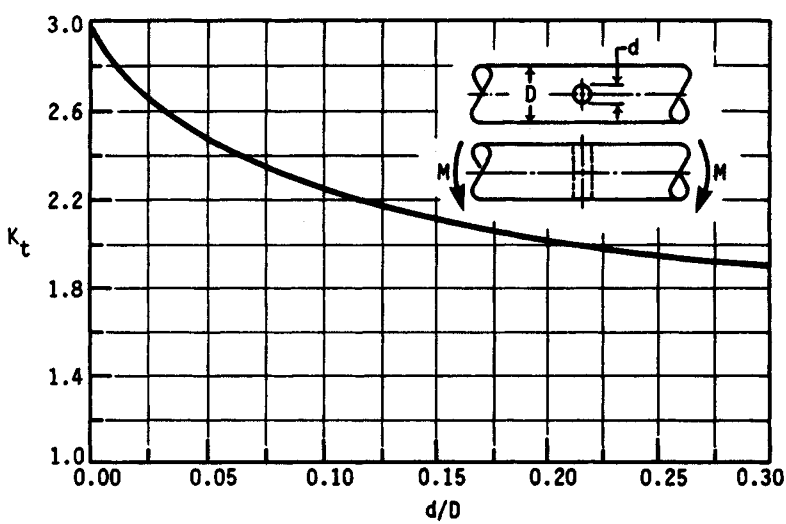

FIGURE 12.13 Round shaft in bending with a transverse hole. $\sigma_o = M/[(\pi D^3/32) - (dD^2/6)]$, approximately. *(From Peterson [12.2].)*

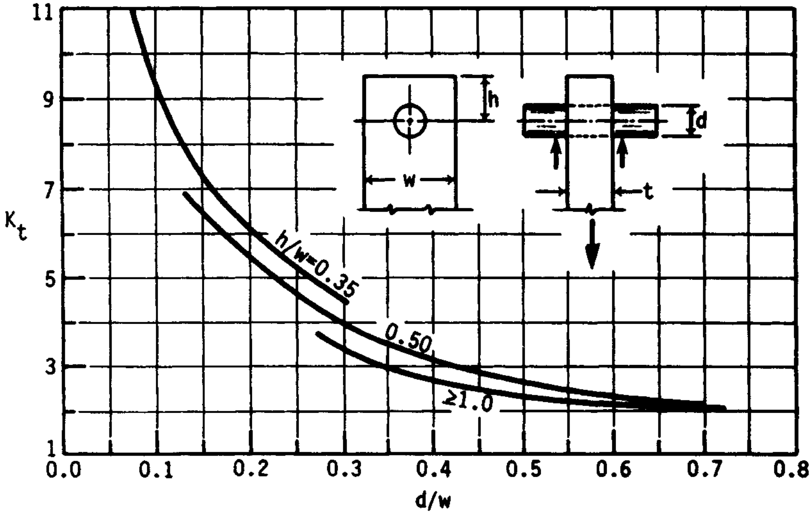

FIGURE 12.14 Plate loaded in tension by a pin through a hole. $\sigma_o = F/A$, where $A = (w - d)t$. When clearance exists, increase K_t by 35 to 50 percent. (*From M. M. Frocht and H. N. Hill, "Stress Concentration Factors around a Central Circular Hole in a Plate Loaded through a Pin in Hole,"* Journal of Applied Mechanics, *vol. 7, no. 1, March 1940, p. A-5, with permission.*)

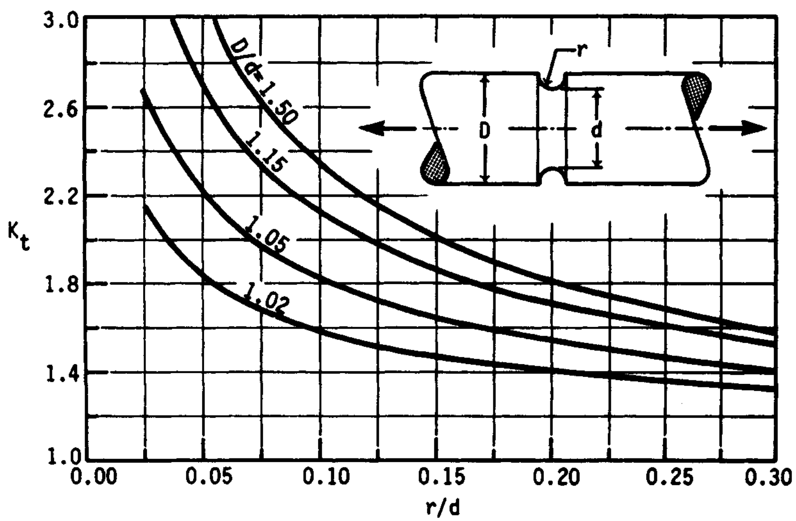

FIGURE 12.15 Grooved round bar in tension. $\sigma_o = F/A$, where $A = \pi d^2/4$. *(From Peterson [12.2].)*

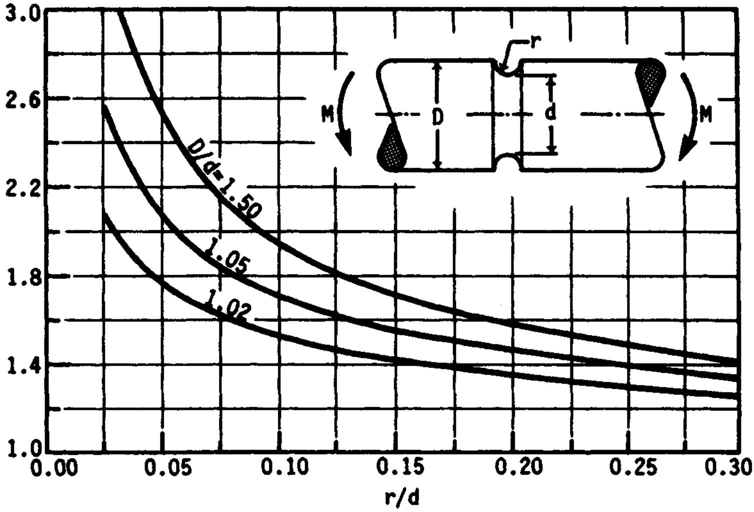

FIGURE 12.16 Grooved round bar in bending. $\sigma_o = Mc/I$, where $c = d/2$ and $I = \pi d^4/64$. *(From Peterson [12.2].)*

12.4.1 Stress Intensities

In Fig. 12.18*a*, suppose the length of the tensile specimen is large compared to the width $2b$. Also, let the crack, of length $2a$, be centrally located. Then a stress-intensity factor K can be defined by the relation

$$K_0 = \sigma(\pi a)^{1/2} \tag{12.8}$$

where σ = average tensile stress. The units of K_0 are kpsi · in$^{1/2}$ or, in SI, MPa · m$^{1/2}$.

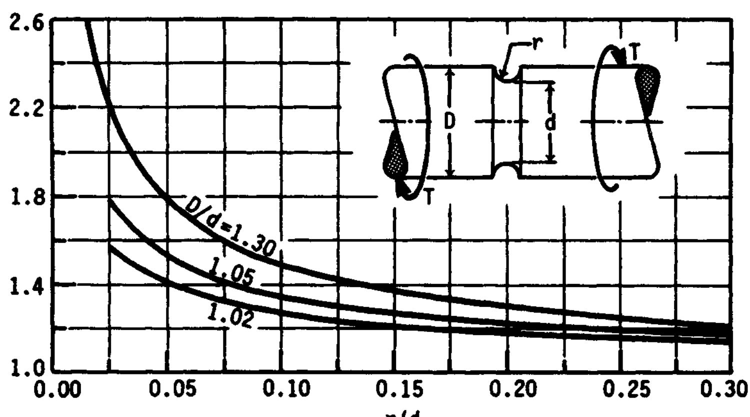

FIGURE 12.17 Grooved round bar in torsion. $\tau_o = Tc/J$, where $c = d/2$ and $J = \pi d^4/32$. *(From Peterson [12.2].)*

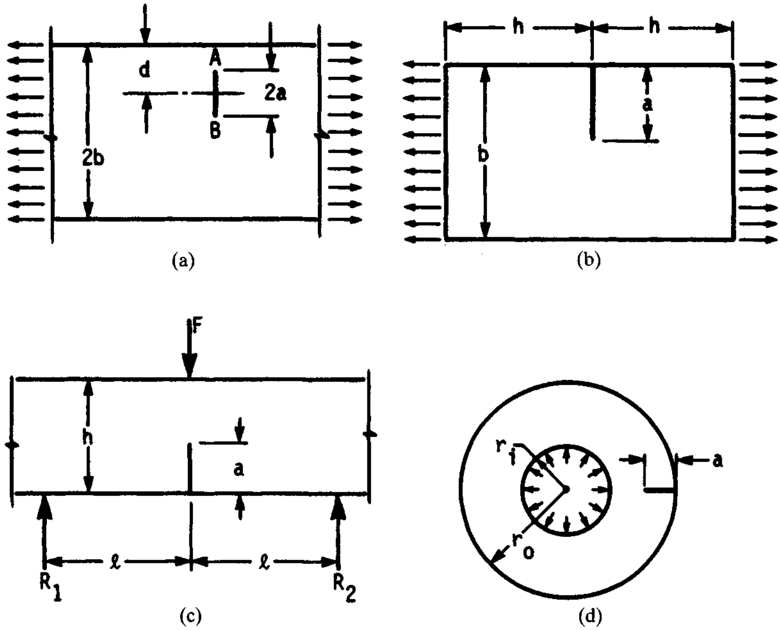

FIGURE 12.18 Typical crack occurrences. (*a*) Bar in tension with interior crack; (*b*) bar in tension with edge crack; (*c*) flexural member of rectangular cross section with edge crack; (*d*) pressurized cylinder with radial edge crack parallel to cylinder axis.

Since the actual value of K for other geometries depends on the loading too, it is convenient to write Eq. (12.8) in the form

$$K_\mathrm{I} = C\sigma(\pi a)^{1/2} \tag{12.9}$$

where

$$C = \frac{K_\mathrm{I}}{K_0} \tag{12.10}$$

Values of this ratio for some typical geometries and loadings are given in Figs. 12.19 and 12.20. Note that Fig. 12.18 must be used to identify the curves on these charts. Additional data on stress-intensity factors can be found in Refs. [12.5], [12.6], and [12.7].

The Roman numeral I used as a subscript in Eq. (12.9) refers to the deformation mode. Two other modes of fracture not shown in Fig. 12.18 are in-plane and out-of-plane shear modes, and these are designated by the Roman numerals II and III. These are not considered here (see Ref. [12.4], p. 262).

12.4.2 Fracture Toughness

When the stress σ of Eq. (12.9) reaches a certain critical value, crack growth begins, and the equation then gives the *critical-stress-intensity factor* K_{Ic}. This is also called the

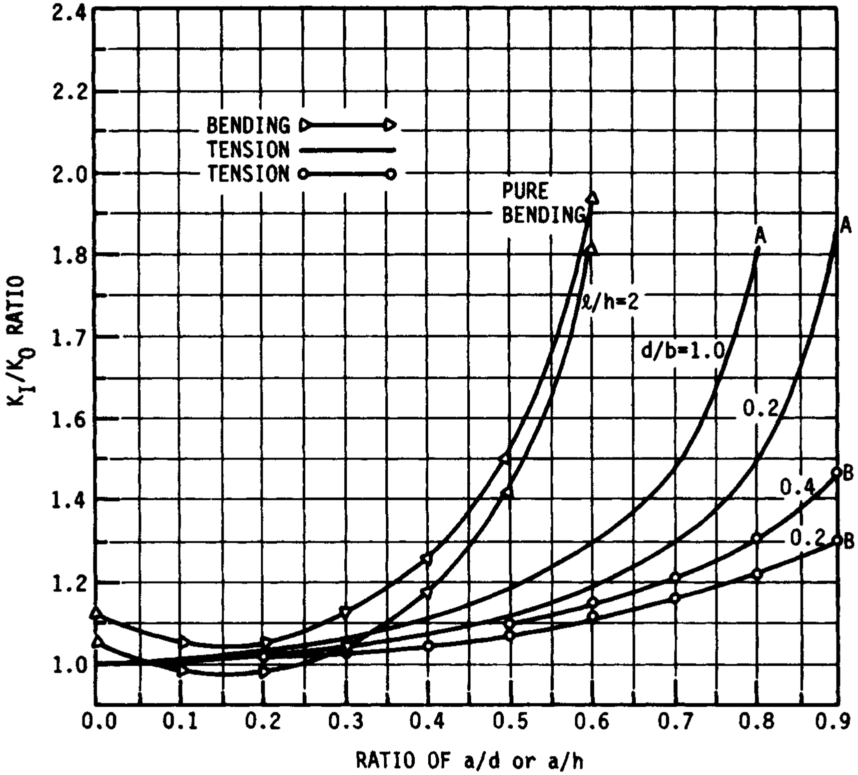

FIGURE 12.19 Stress-intensity charts for cracks shown in Fig. 12.18*a* and *c*. Letters *A* and *B* identify the ends of the crack shown in Fig. 12.18*a*. Values of $\ell/h > 2$ will produce curves closer to the curve for pure bending.

fracture toughness. Since it is analogous to strength, we can define design factor as

$$n = \frac{K_c}{K} \tag{12.11}$$

Some typical values of K_c are given in Table 12.1. For other materials, see Ref. [12.8].

12.5 NONFERROUS METALS

Designing for static loads with aluminum alloys is not much different from designing for the steels. Aluminum alloys, both cast and wrought, have strengths in tension and compression that are about equal. The yield strengths in shear vary from about 55 to 65 percent of the tensile yield strengths, and so the octahedral shear theory of failure is valid.

The corrosion resistance (see Chap. 44), workability, and weldability obtainable from some of the alloys make this a very versatile material for design. And the extrusion capability means that a very large number of wrought shapes are available.

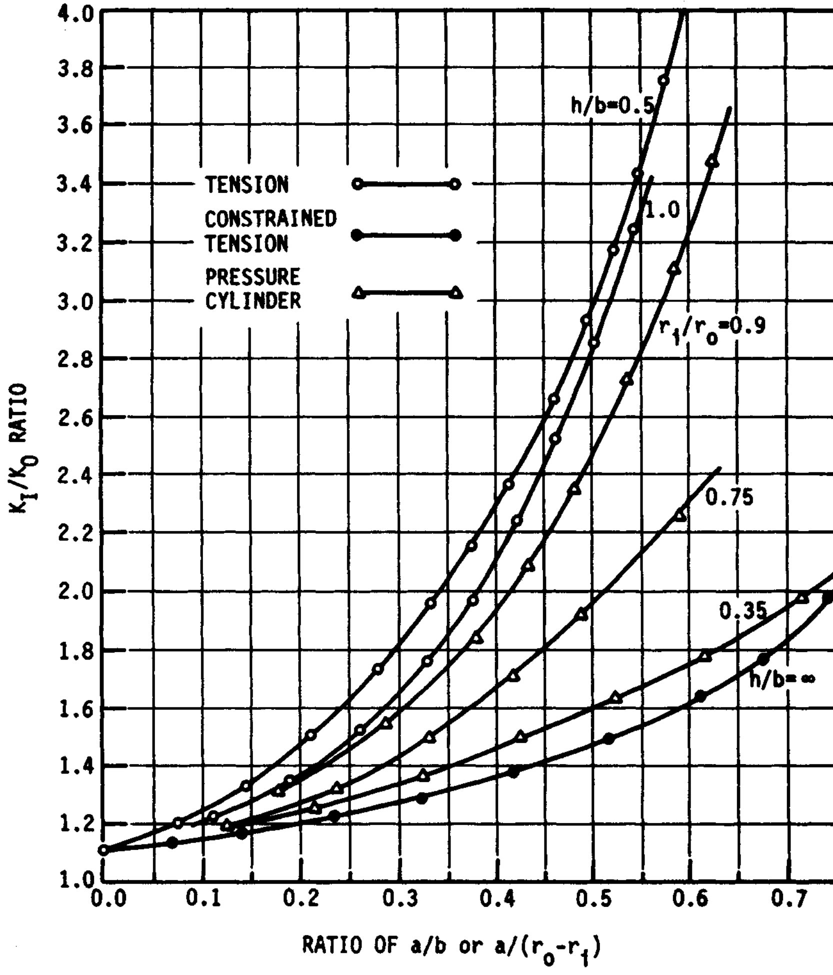

FIGURE 12.20 Stress-intensity chart for cracks shown in Figs. 12.18*b* and *d*. The curve $h/b = \infty$ has bending constraints acting on the member.

However, these alloys do have a temperature problem, as shown by the curves of strength versus temperature in Fig. 12.21. Other aluminum alloys will exhibit a similar characteristic.

Alloying elements used with copper as the base element include zinc, lead, tin, aluminum, silicon, manganese, phosphorus, and beryllium. Hundreds of variations in the percentages used are possible, and consequently, the various copper alloys may have widely differing properties. The primary consideration in selecting a copper alloy may be the machinability, ductility, hardness, temperature properties, or corrosion resistance. Strength is seldom the primary consideration. Because of these variations in properties, it is probably a good idea to consult the manufacturer concerning new applications until a backlog of experience can be obtained.

TABLE 12.1 Values of the Fracture Toughness K_{Ic} for a Few Engineering Materials

Material	Designation	UNS no.	Yield strength		Fracture toughness	
			MPa	kpsi	MPa·m$^{1/2}$	kpsi·in$^{1/2}$
Aluminum	2024-T851	A92094-T851	455	66	26	24
	7075-T651	A97075-T651	495	72	24	22
Titanium	Ti-6AL-4V	R56401	910	132	115	105
	Ti-6AL-4V	R56401	1035	150	55	50
Steel	AISI 4340	G43400	860	125	99	90
	AISI 4340	G43400	1515	220	60	55
	AISI 52100	G52986	2070	300	14	13

SOURCE: Professor David K. Felbeck, The University of Michigan, by personal communication.

Magnesium alloys have a weight about two-thirds that of aluminum and one-fourth that of steel. Magnesium alloys are not very strong and are characterized by having a compressive strength that is somewhat less than the tensile strength. They are also so sensitive to temperature that they are weakened even by contact with boiling water.

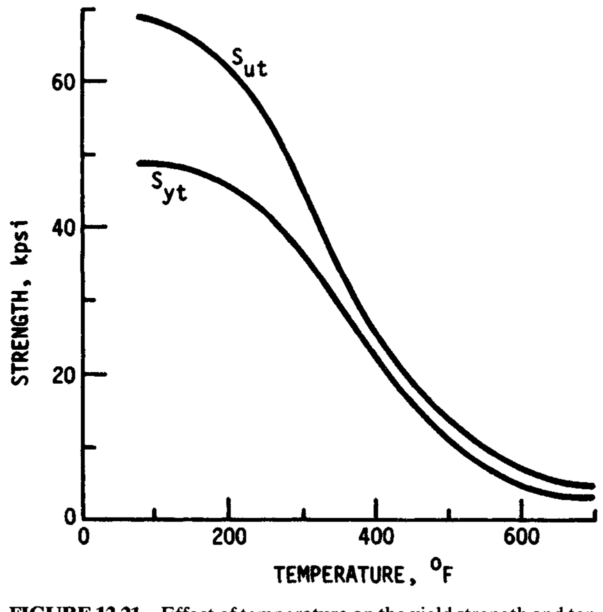

FIGURE 12.21 Effect of temperature on the yield strength and tensile strength of aluminum alloy A92024-T4. *(ALCOA.)*

12.6 STOCHASTIC CONSIDERATIONS

It is helpful to understanding to recall the nature of deterministic theories of failure. All the stresses at a point are consequences of geometry and loading. In linear systems, all the stresses at a point are proportional to load. If there is variability in load, there is variability in the stresses at a point. When variability in geometry can be ignored compared to variability in loading, the distribution type and the coefficients of variation agree in both stress and load. In a deterministic theory of failure, such as distortion energy, the von Mises σ' is set equal to the loss-of-function stress called yield strength S_y, or to S_y/n. One cannot do this directly with stochastic variables. The distribution type of the von Mises stress is that of the load, and is independent of the distribution type of the yield strength. An equation such as Eq. (12.3) can be constructed only for the approximate relationship of the means (strictly, the medians).

In examining histograms obtained in yield strength testing, normal, lognormal, and Weibull fits can be successful. The coefficient of variation averages 0.064 for yield strengths of 31 steels that differ in composition or thermomechanical treatment, and the range is 0.02 to 0.10. More data can be found in Ref. [12.9]. The dispersion is wider than that of the corresponding ultimate tensile strength, which averages 0.047 and ranges from 0.017 to 0.077; this may be due in part to testing methodology differences.

Since one often encounters lognormal loading and yield strength, Eq. (2.6), with $S = S_y$, the yield strength, and $\sigma = \sigma'$, the von Mises stress, is usefully written as

$$C_n = \sqrt{C_{S_y}^2 + C_{\sigma'}^2} = \sqrt{C_{S_y}^2 + C_P^2}$$

where $\mathbf{P}$ is the load causing $\boldsymbol{\sigma}'$. It follows that

$$\bar{n} = \exp\left[-z\sqrt{\ln(1 + C_n^2)} + \ln\sqrt{1 + C_n^2}\right] \doteq \exp\left[C_n(-z + C_n/2)\right]$$

and Eq. (12.3) can now be expressed as

$$\bar{\sigma}' = \frac{\bar{S}_y}{\bar{n}}$$

If reliability is sought, Eqs. (2.5) and (2.4) can be used.

REFERENCES

12.1 R. E. Peterson, *Stress Concentration Factors,* John Wiley & Sons, New York, 1974.

12.2 R. E. Peterson, "Design Factors for Stress Concentration," *Machine Design,* vol. 23, no. 2, p. 161; no. 5, p. 159; no. 6, p. 173; no. 7, p. 155; 1951.

12.3 G. M. Kurajian and D. J. West, "Stress Concentration Factor Determination in Stepped Hollow Shafts," *Failure Prevention and Reliability,* American Society of Mechanical Engineers, New York, 1977.

12.4 R. W. Hertzberg, *Deformation and Fracture Mechanics of Engineering Materials,* John Wiley & Sons, New York, 1976.

12.5 H. Tada, P. C. Paris, and G. R. Irwin, *The Stress Analysis of Cracks Handbook,* Del Research, Hellertown, Pa., 1973.

12.6 G. C. M. Sih, *Handbook of Stress Intensity Factors,* Lehigh University, Bethlehem, Pa., 1973.

12.7 D. P. Rooke and D. J. Cartwright, *Compendium of Stress Intensity Factors,* Hillingdon Press, Uxbridge, England, 1976.

12.8 *Damage Tolerant Handbook,* Metals and Ceramics Information Center, Battelle, Columbus, Ohio, 1975.

12.9 C. R. Mischke, "Some Property Data and Corresponding Weibull Parameters for Stochastic Mechanical Design, *Transactions of A.S.M.E., Journal of Mechanical Design,* vol. 114, March 1992, pp. 29–34.